

Modeling Blazar SEDs and Spectral Variability with Time-Dependent Diffusive Shock Acceleration: Application to 1ES 1959+650 Observed with AstroSAT

Markus Böttcher

North-West University

Potchefstroom, South Africa



Matthew Baring (Rice University, Houston, TX, USA)

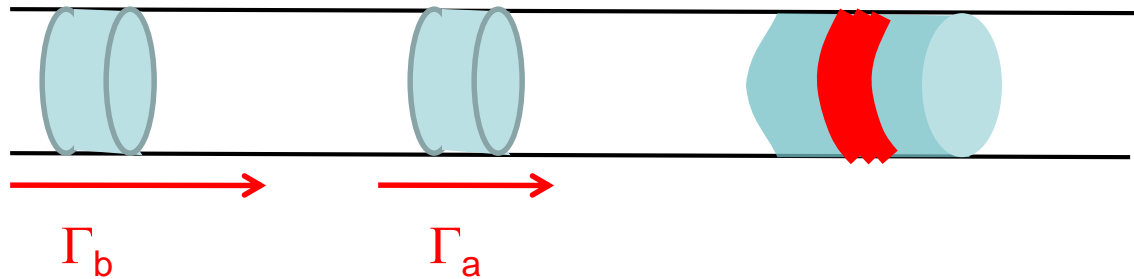
Sunil Chandra (NWU, Potchefstroom, South Africa + SAAO)

Based on Böttcher & Baring (2019): ApJ, 887, 133 (arXiv:1911.02834)
+ Chandra et al. (2021): ApJ, submitted

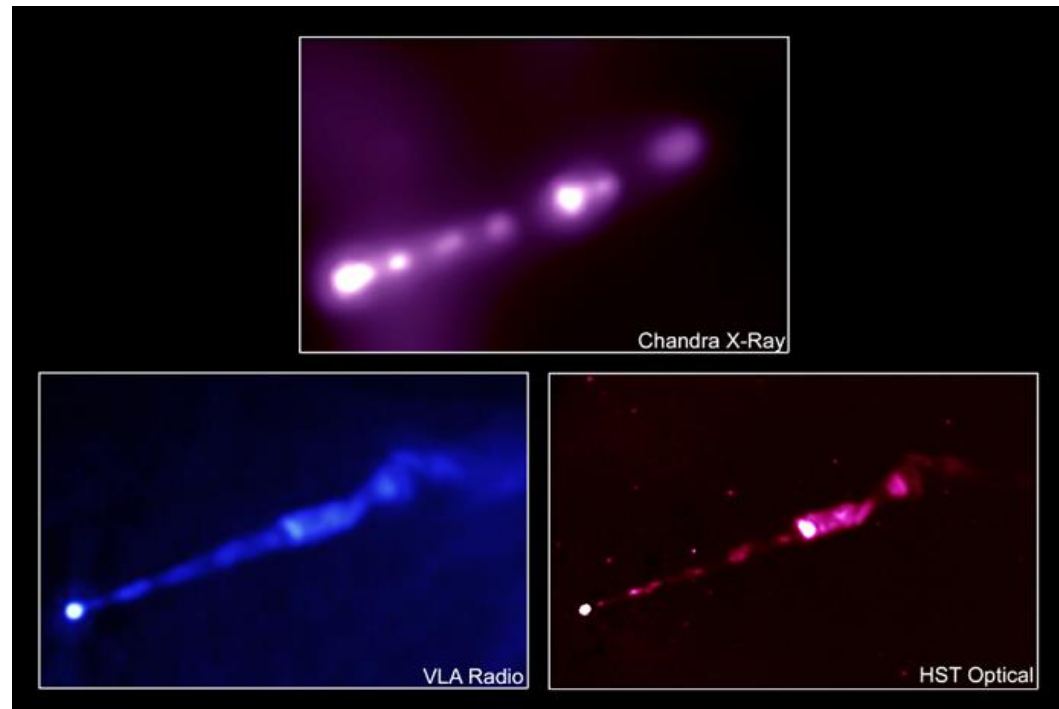


Supported by the South African Research Chairs Initiative (SARChI) of the Department of Science and Technology and the National Research Foundation of South Africa.

Relativistic Shocks in Jets



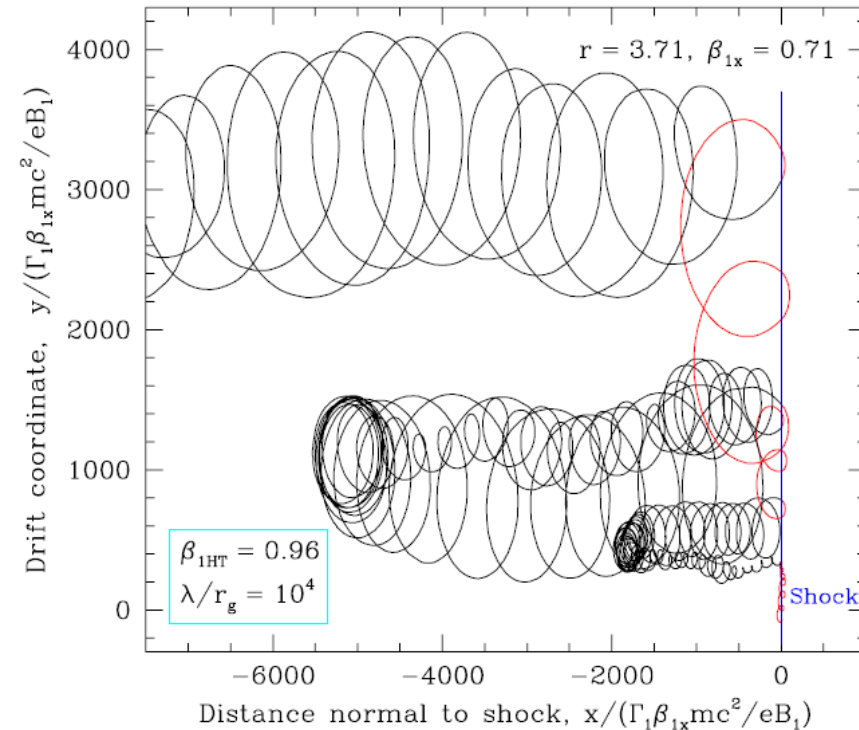
- Internal Shocks: likely sites of relativistic particle acceleration.
- Most likely mildly relativistic, $\beta\gamma \sim 1$
- In most works: Simple power-law or log-parabola electron spectra (from Fermi I / II acceleration) assumed with spectral index (~ 2) put in “by hand”.



Jet of M87 at different wavelengths

Monte-Carlo Simulations of Diffusive Shock Acceleration (DSA)

- Gyration in B-fields and diffusive transport (pitch-angle diffusion) modeled by a Monte Carlo technique.
- Shock crossings produce net energy gains \rightarrow first-order Fermi.

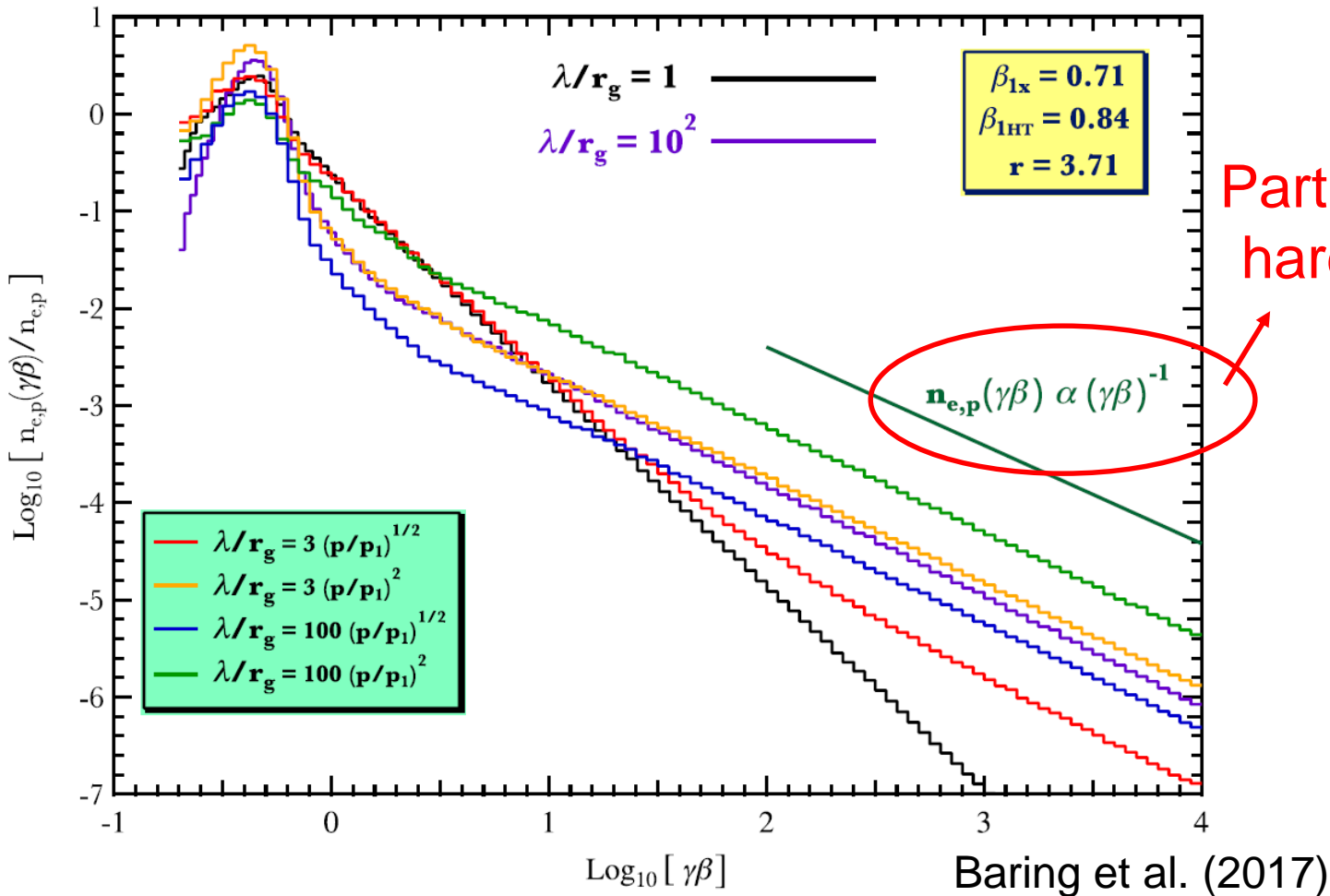


(Summerlin & Baring 2012)

- Pitch-angle diffusion parameterized through a mean-free-path (λ_{pas}) parameter η (p):

$$\lambda_{pas} = \eta(p) * r_g \sim p^\alpha \quad (\alpha \geq 1)$$

Shock Acceleration Spectra



Non-thermal particle spectral index and thermal-to-non-thermal normalization are strongly dependent on η_0 , α , and B-field obliquity!

Constraints from Blazar SEDs

Synchrotron peak $\leftrightarrow \gamma_{\max}$

Balance $t_{\text{acc}} \sim \eta(\gamma) \omega_{\text{gyr}}(\gamma)^{-1}$
with radiative cooling time scale

If synchrotron cooling dominates:

$$\gamma_{\max} \sim B^{-1/2} [\eta(\gamma_{\max})]^{-1/2}$$

$$\Rightarrow h\nu_{\text{sy}} \sim 100 \delta [\eta(\gamma_{\max})]^{-1} \text{ MeV} \quad (\text{independent of B-field!})$$

Constraints from Blazar SEDs

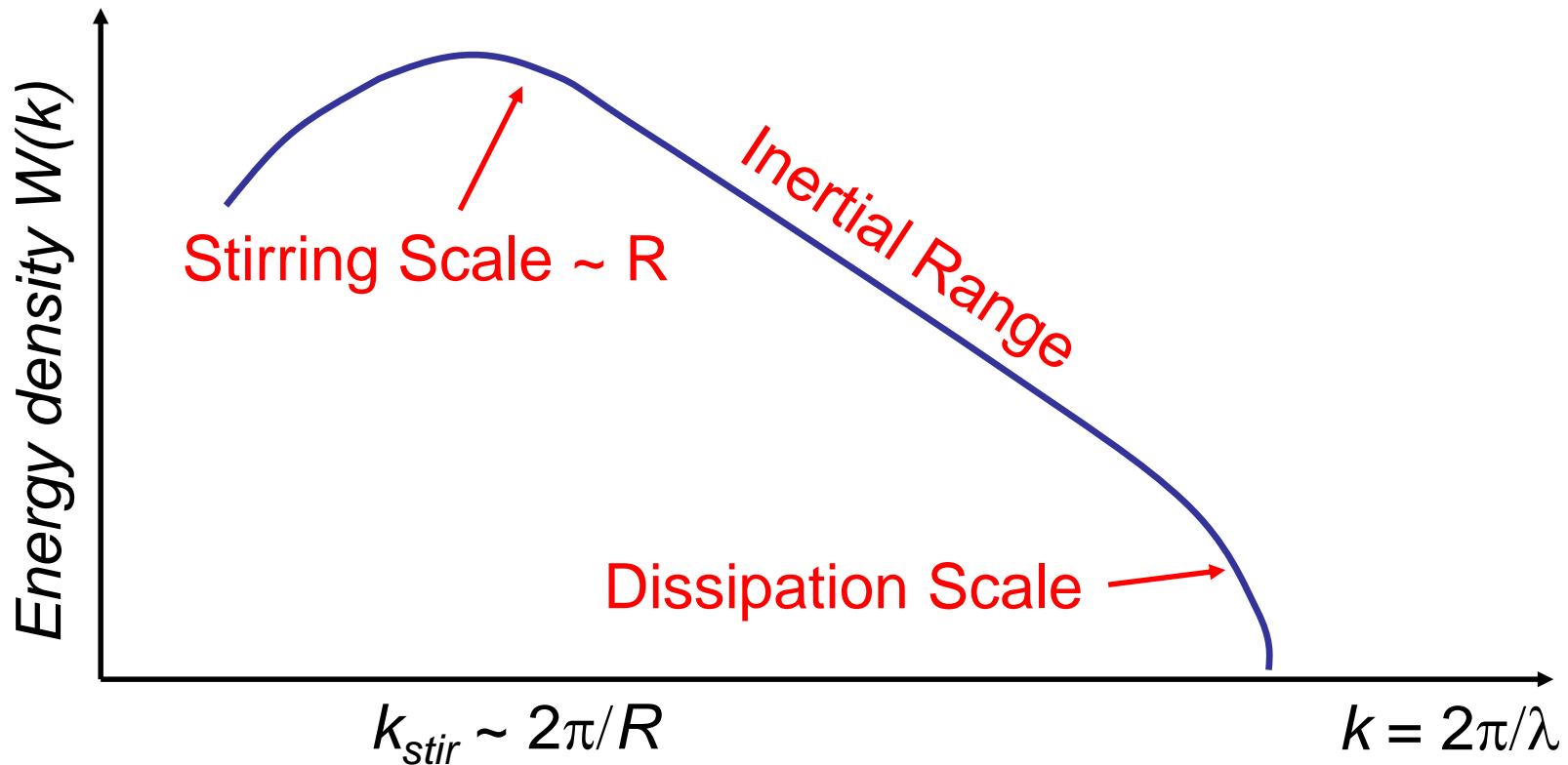
$$h\nu_{\text{sy}} \sim 100 \delta [\eta(\gamma_{\text{max}})]^{-1} \text{ MeV} \quad (\text{independent of B-field!})$$

- ⇒ Need large $\eta(\gamma_{\text{max}})$ to obtain synchrotron peak in optical/UV/X-rays
- ⇒ But: Need moderate $\eta(\gamma \sim 1)$ for efficient injection of particles into the non-thermal accelerations scheme
- ⇒ Need strongly energy dependent pitch-angle scattering m.f.p., with $\alpha > 1$ (Baring et al. 2017)

Implications for Shock-Induced Turbulence

Gyro-resonance condition: $\lambda_{\text{res}} \propto \rho$

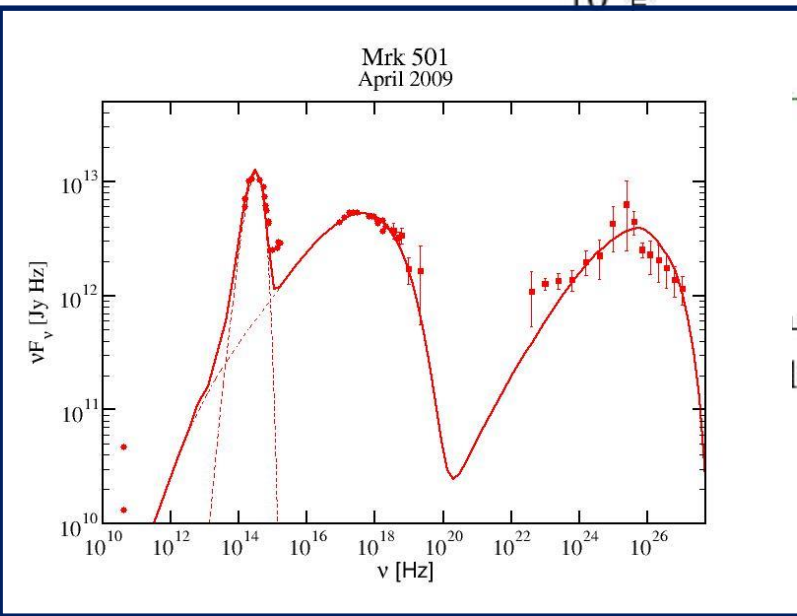
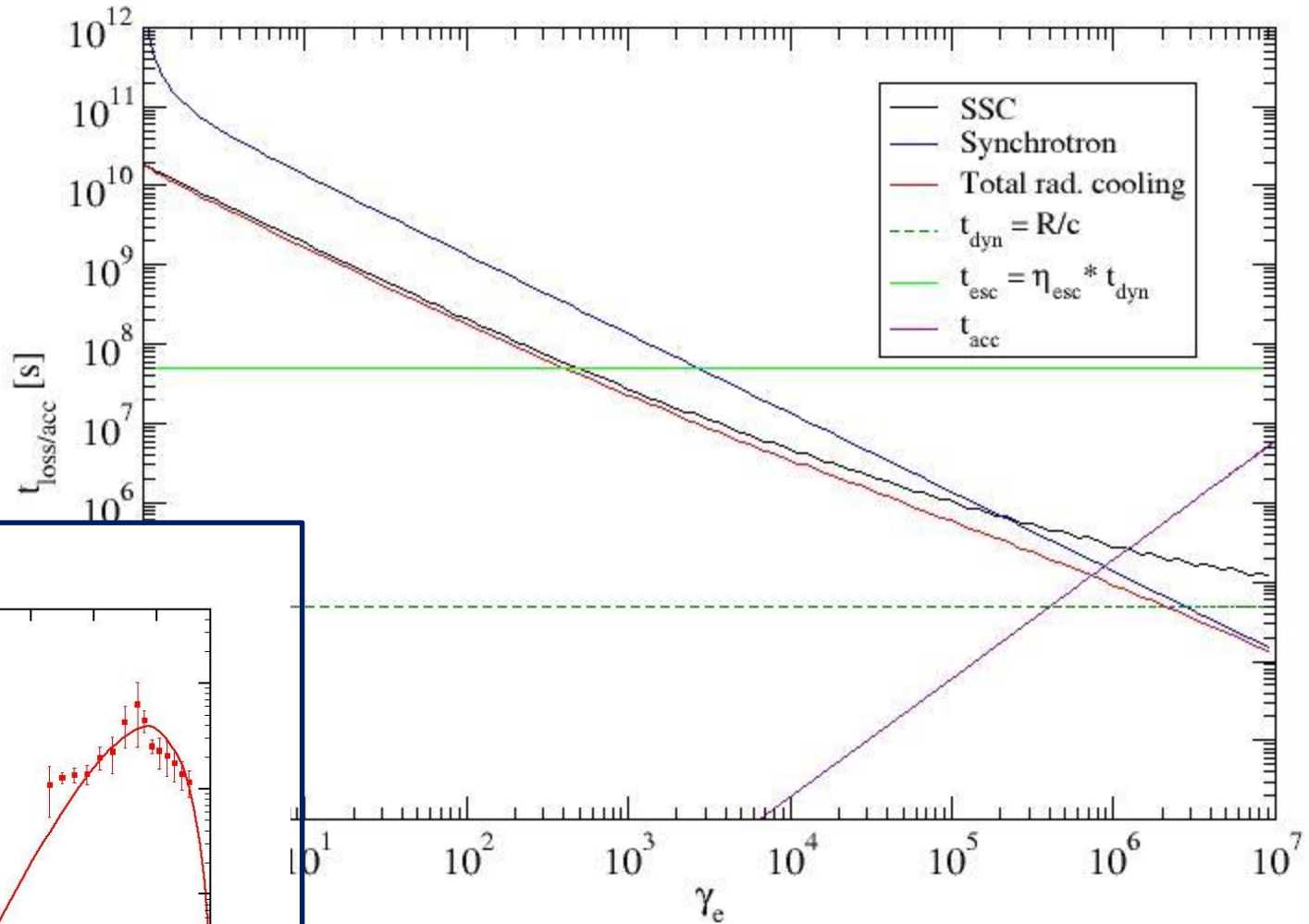
=> Higher-energy particles interact with longer-wavelength turbulence



Turbulence level decreasing with increasing distance from the shock
=> High-energy (large r_g) particles “see” reduced turbulence
=> Large λ_{pas}

Electron Evolution Time Scales

Mrk 501



Time-Dependent Electron Evolution with Radiative Energy Losses

Acceleration time scale:

$$t_{acc} = \eta t_{gyr} = \eta \frac{2\pi \gamma m_e c}{eB} \ll t_{cool}, t_{dyn}$$

For almost all electrons

⇒ Use shock-accelerated electron spectrum as instantaneous injection $Q_e(\gamma)$;

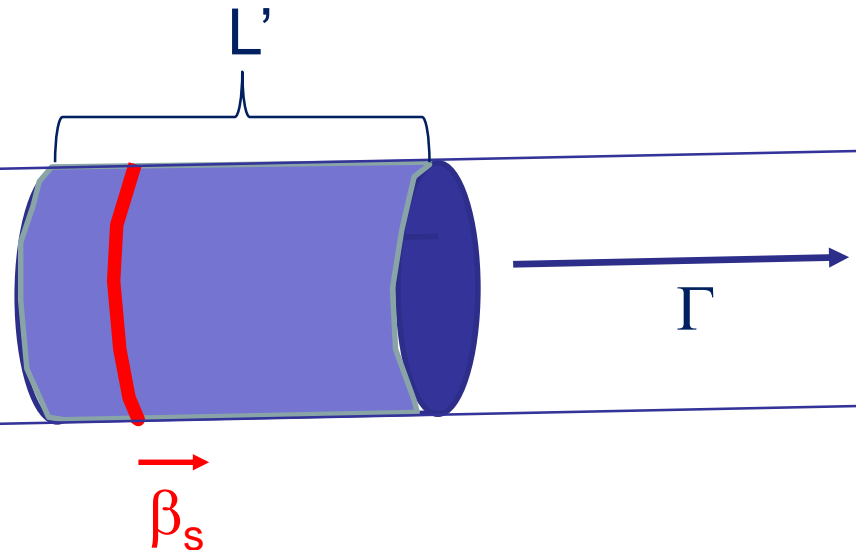
⇒ Solve Fokker-Planck Equation for electrons:

$$\frac{\partial n_e(\gamma, t)}{\partial t} = - \frac{\partial}{\partial \gamma} (\dot{\gamma} n_e) + Q_e(\gamma, t) - \frac{n_e(\gamma, t)}{t_{esc, e}}$$

Numerical Scheme

- Injection spectra from turbulence characteristics + MC simulations of DSA
- Injection from small acceleration zone (shock) into larger radiation zone
- Time-dependent leptonic code based on Böttcher & Chiang (2002)
- Radiative processes:
 - Synchrotron
 - Synchrotron self-Compton (SSC)
 - External Compton (EC: dust torus + BLR + direct accretion disk)

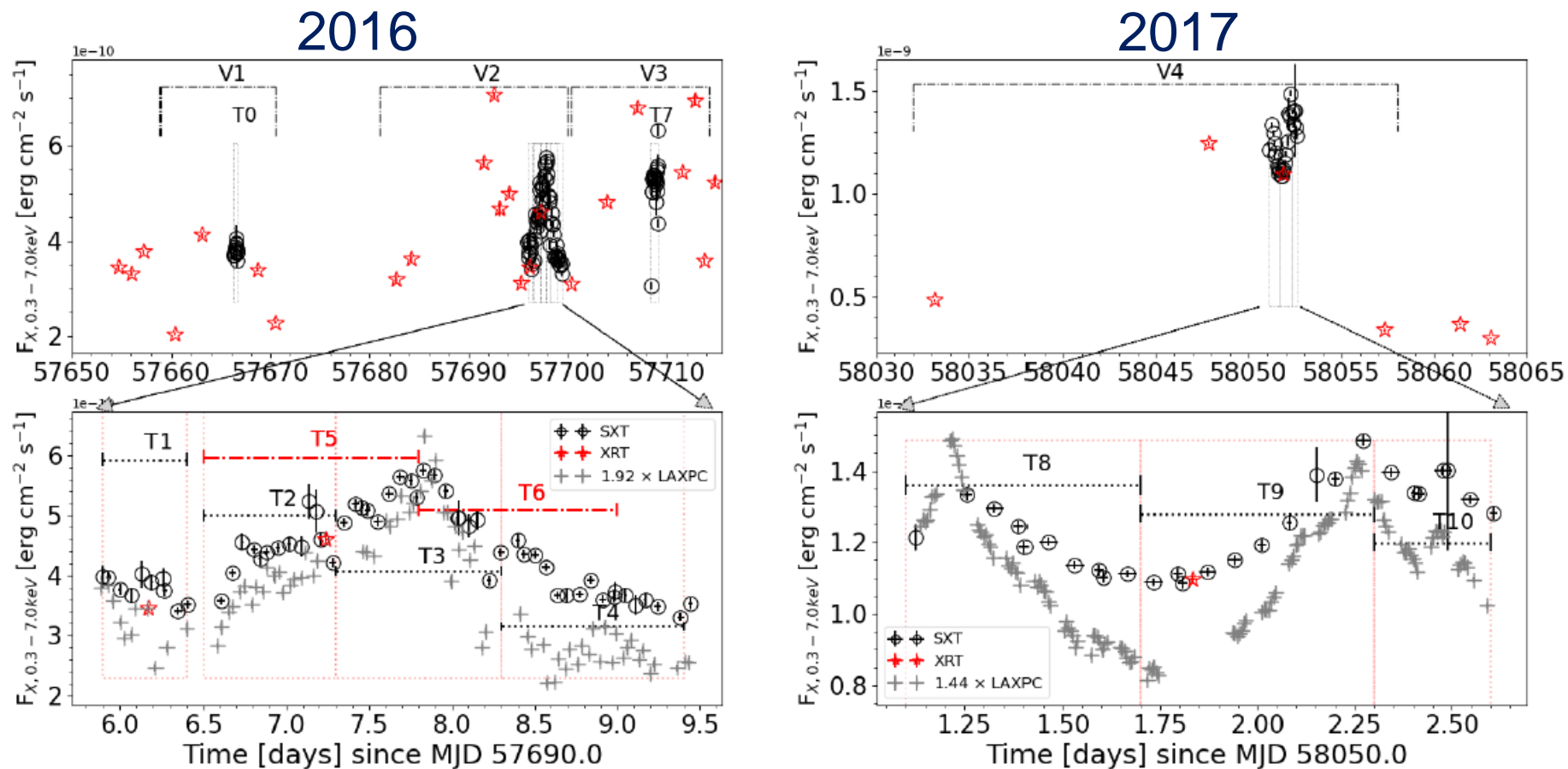
Shock injection “on” for
 $0 < \Delta t' < L'/v'_s$



$$Q_{e,s}(\gamma, t') = Q_{e,s}(\gamma) H(t'; 0, \Delta t')$$

Example: HBL 1ES 1959+650

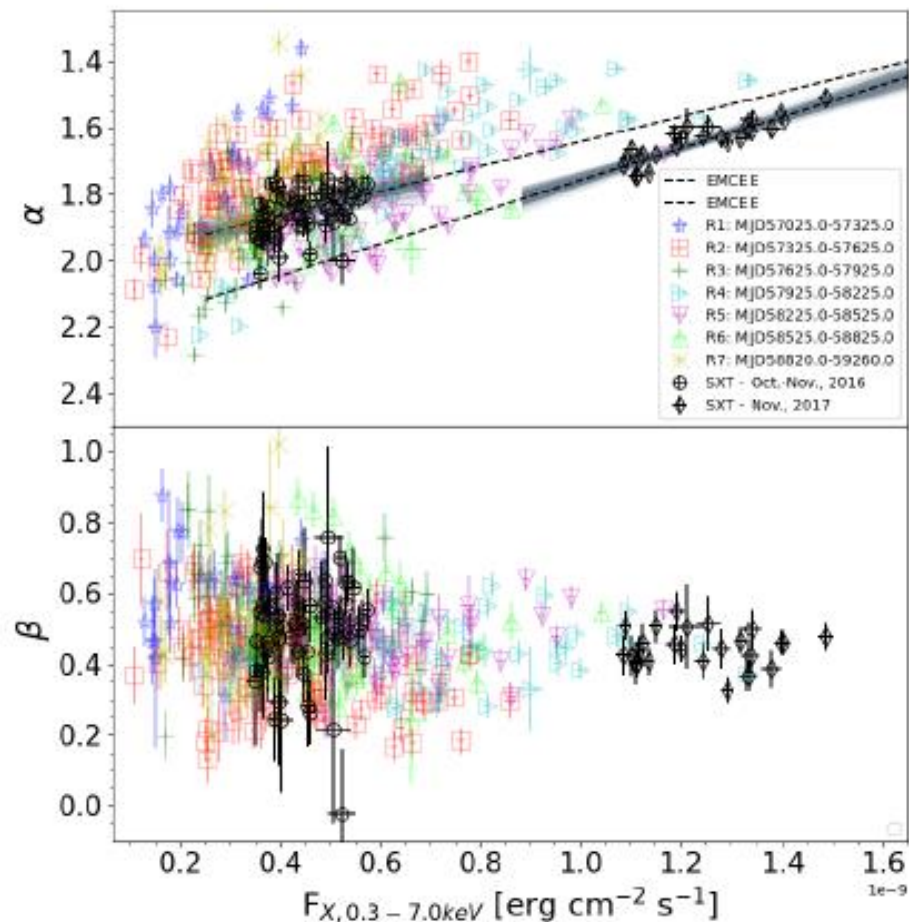
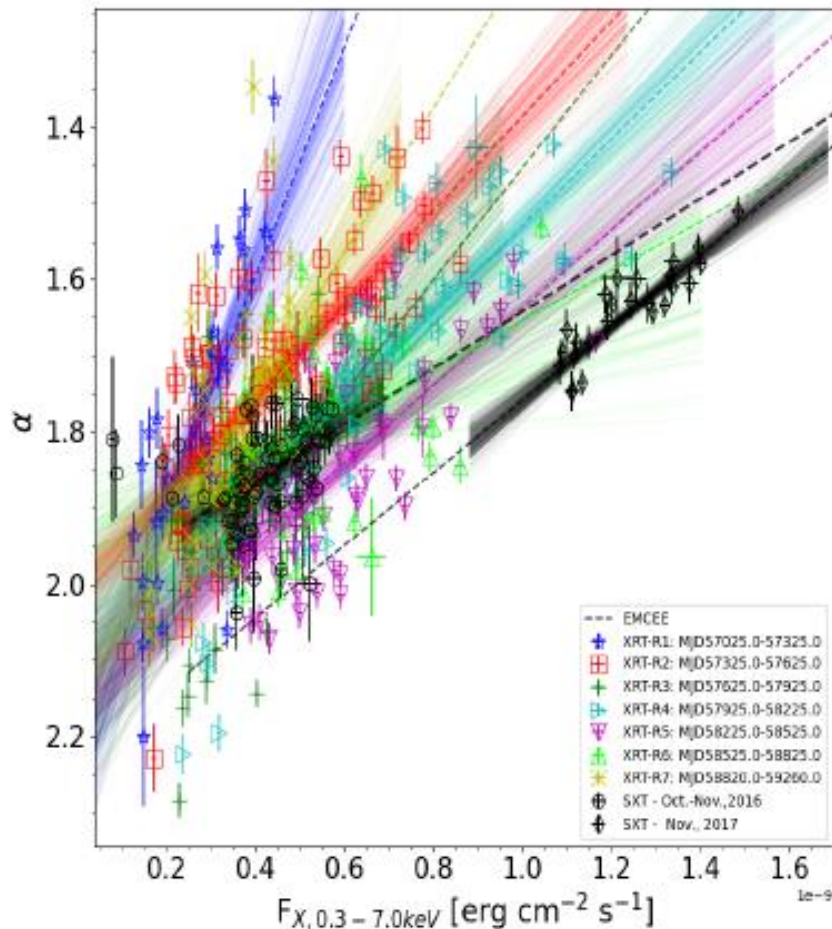
- Prototypical HSP BL Lac object at $z = 0.048$
- Observed with AstroSAT during flaring states in 2 long (144 ksec) observations in 2016 and 2017



(Chandra et al. 2021)

Example: HBL 1ES 1959+650

- Pronounced spectral variability (harder when brighter)
- Log-parabolic spectral fits: $F_E \sim E^{-(\alpha + \beta \log[E/E_0])}$



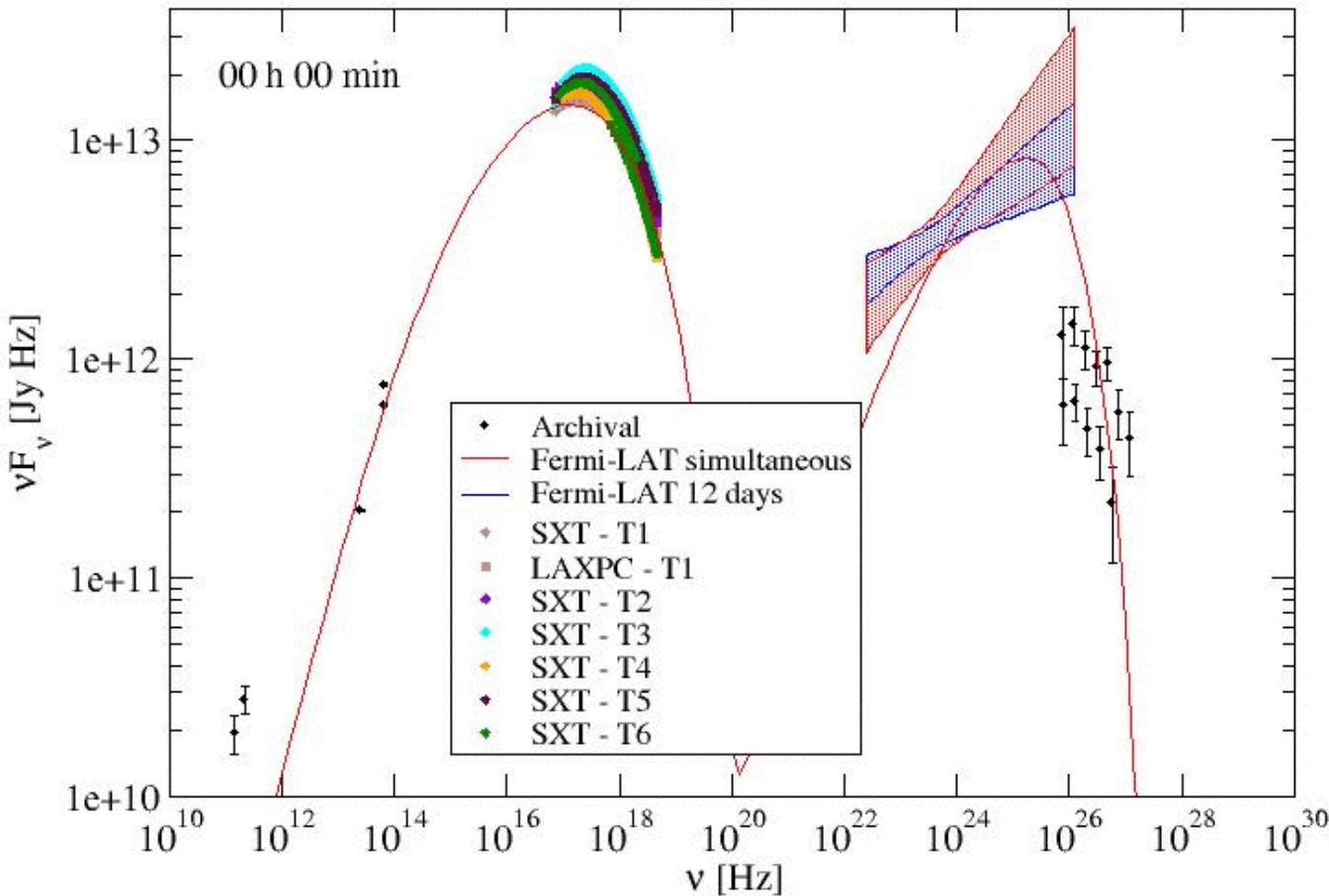
(Chandra et al. 2021)

1ES 1959+650 in 2016

Complex variability patterns require passage of multiple shocks.

1ES 1959+650
2016

$$\lambda_{\text{pas}} = 60 r_g \gamma^{0.9}$$



(Chandra et al. 2021)

$$\eta_1 = 60$$

$$\alpha = 1.9$$

$$B = 0.15 \text{ G}$$

$$\delta = 20$$

$$R = 6 \cdot 10^{15} \text{ cm}$$

$$\rightarrow \Delta t' \sim 2 \cdot 10^5 \text{ s}$$

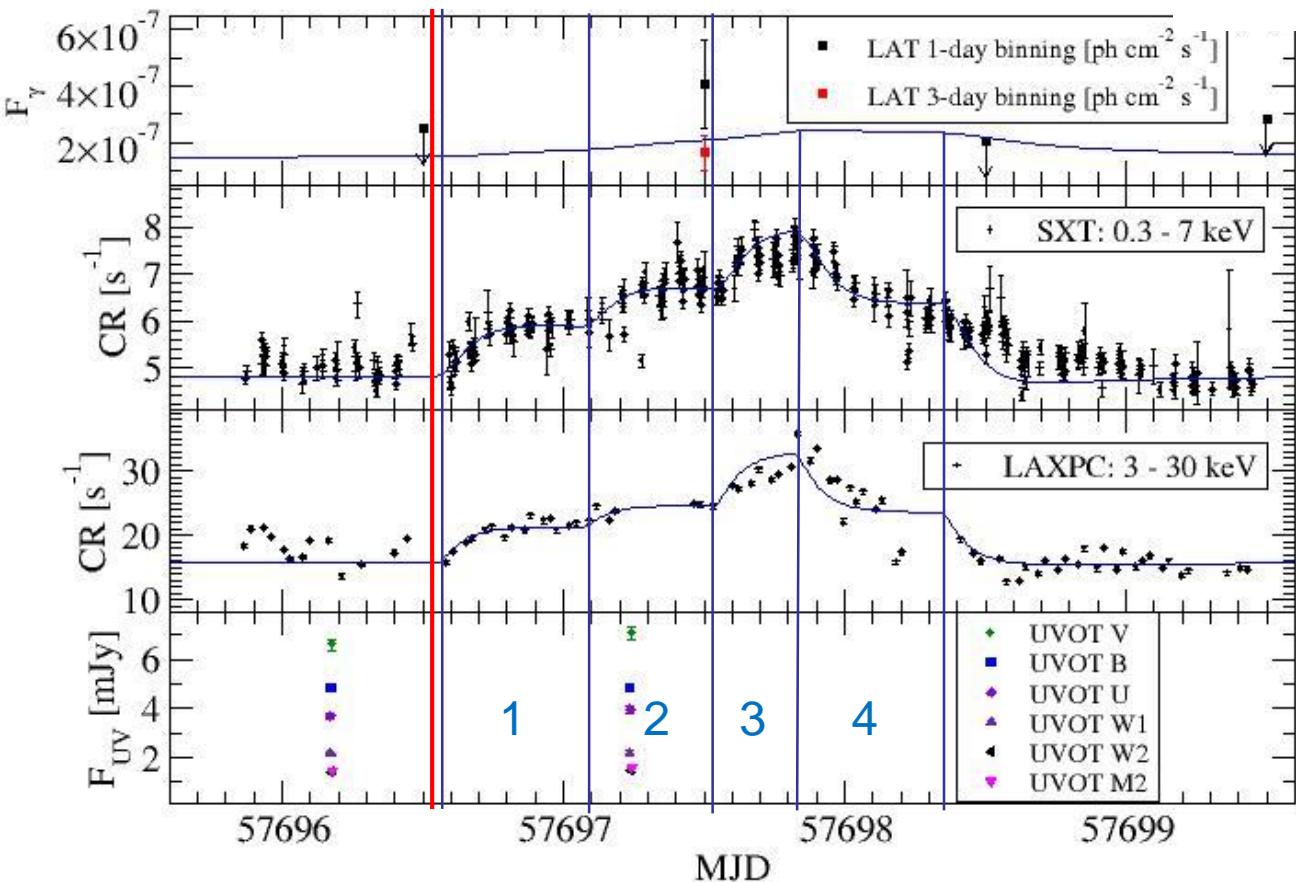
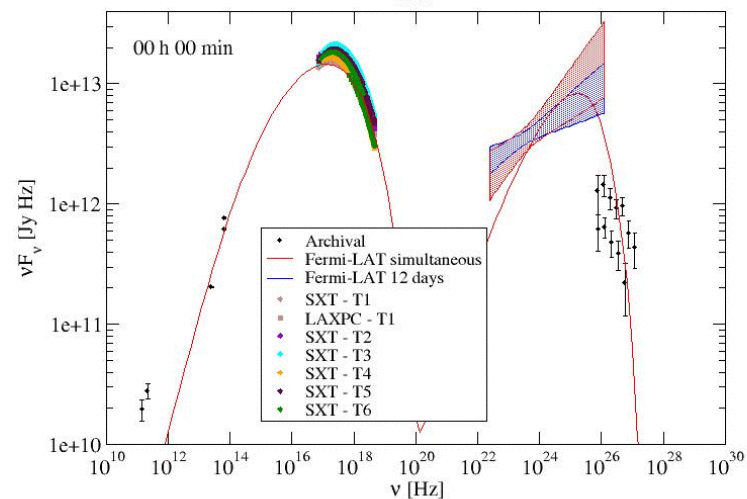
$$\rightarrow \Delta t_{\text{obs}} \sim 2.8 \text{ h}$$

Flaring caused by

- increasing L_{inj}
- decreasing η_0

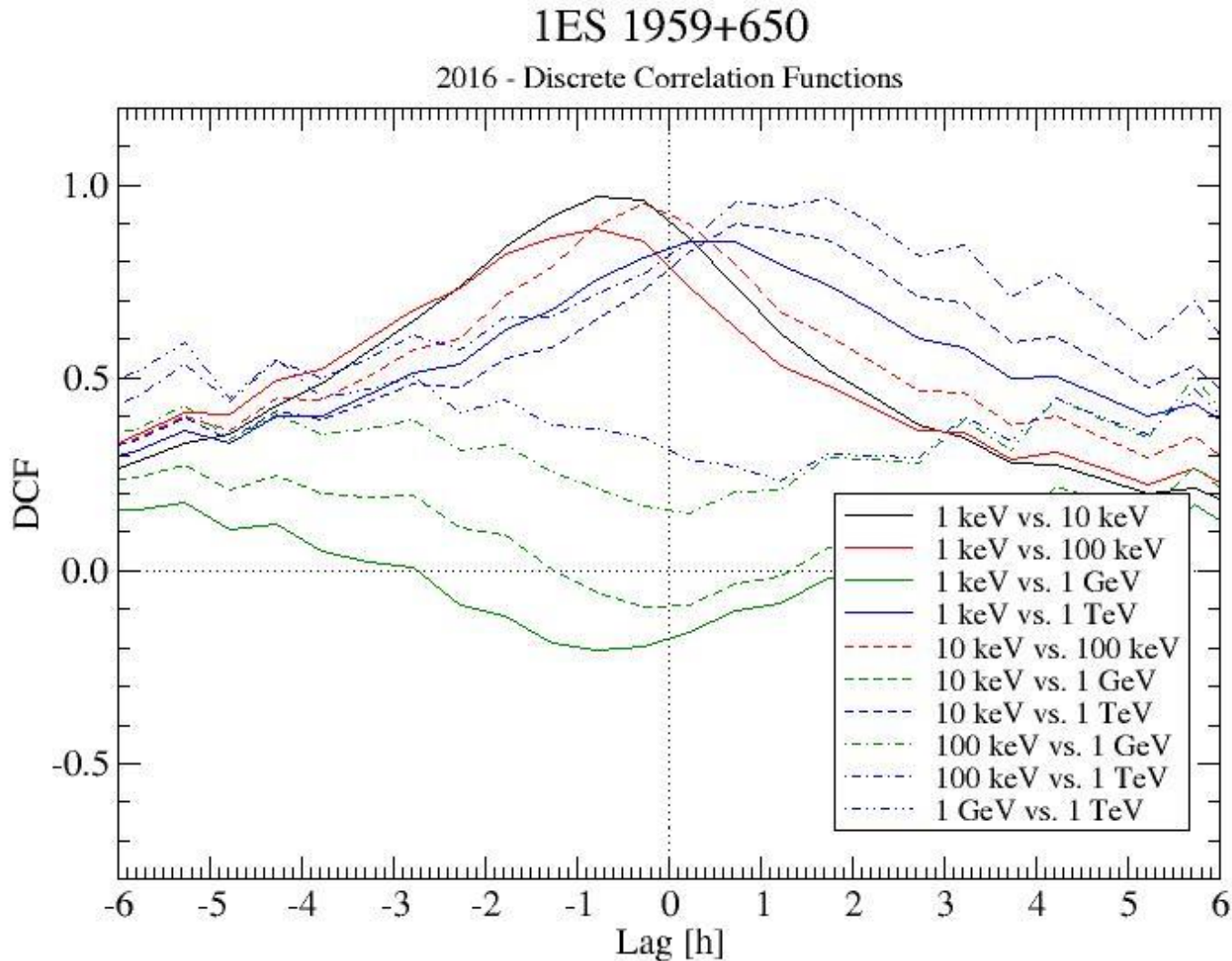
2016: MWL Light Curves

Parameter [units]	L_{inj} [erg/s]	η_0	α
Quiescence	2.5×10^{40}	60	1.9
Shock 1	3.0×10^{40}	50	1.9
Shock 2	3.5×10^{40}	50	1.9
Shock 3	4.1×10^{40}	40	1.9
Shock 4	3.4×10^{40} <td>50</td> <td>1.9</td>	50	1.9



(Chandra et al. 2021)

2016: Discrete Correlation Functions



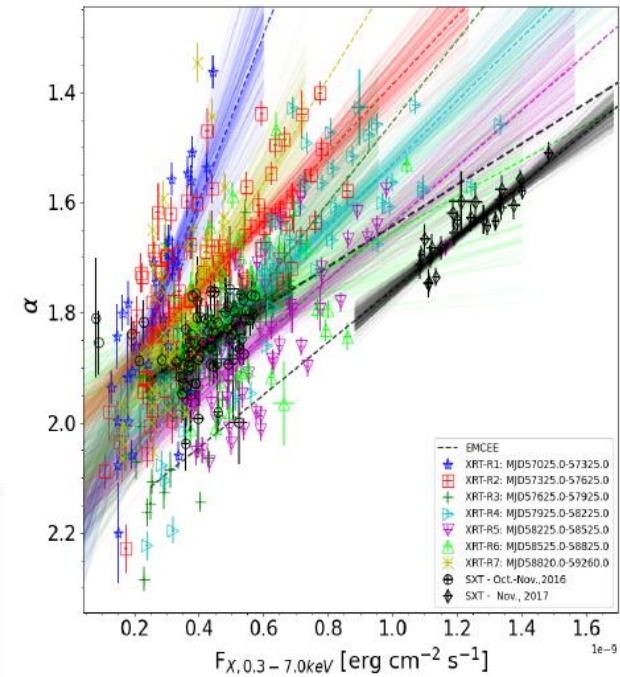
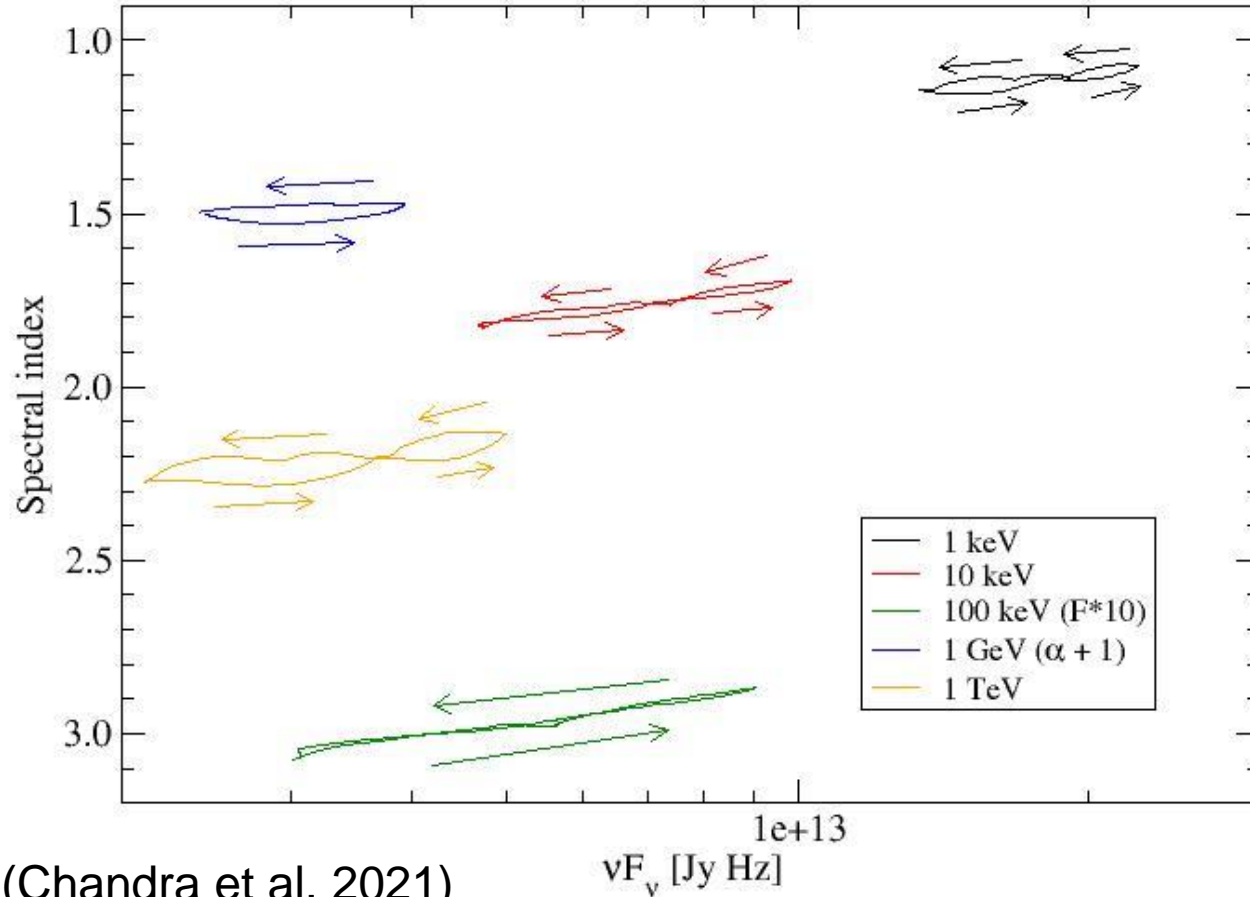
Strong correlations between X-rays and VHE γ -rays

Soft X-ray lags of ~ 1 hour behind hard X-rays and VHE γ -rays.

(Chandra et al. 2021)

2016: Hardness-Intensity Diagrams

1ES 1959+650
2016 - Hardness-Intensity Diagrams



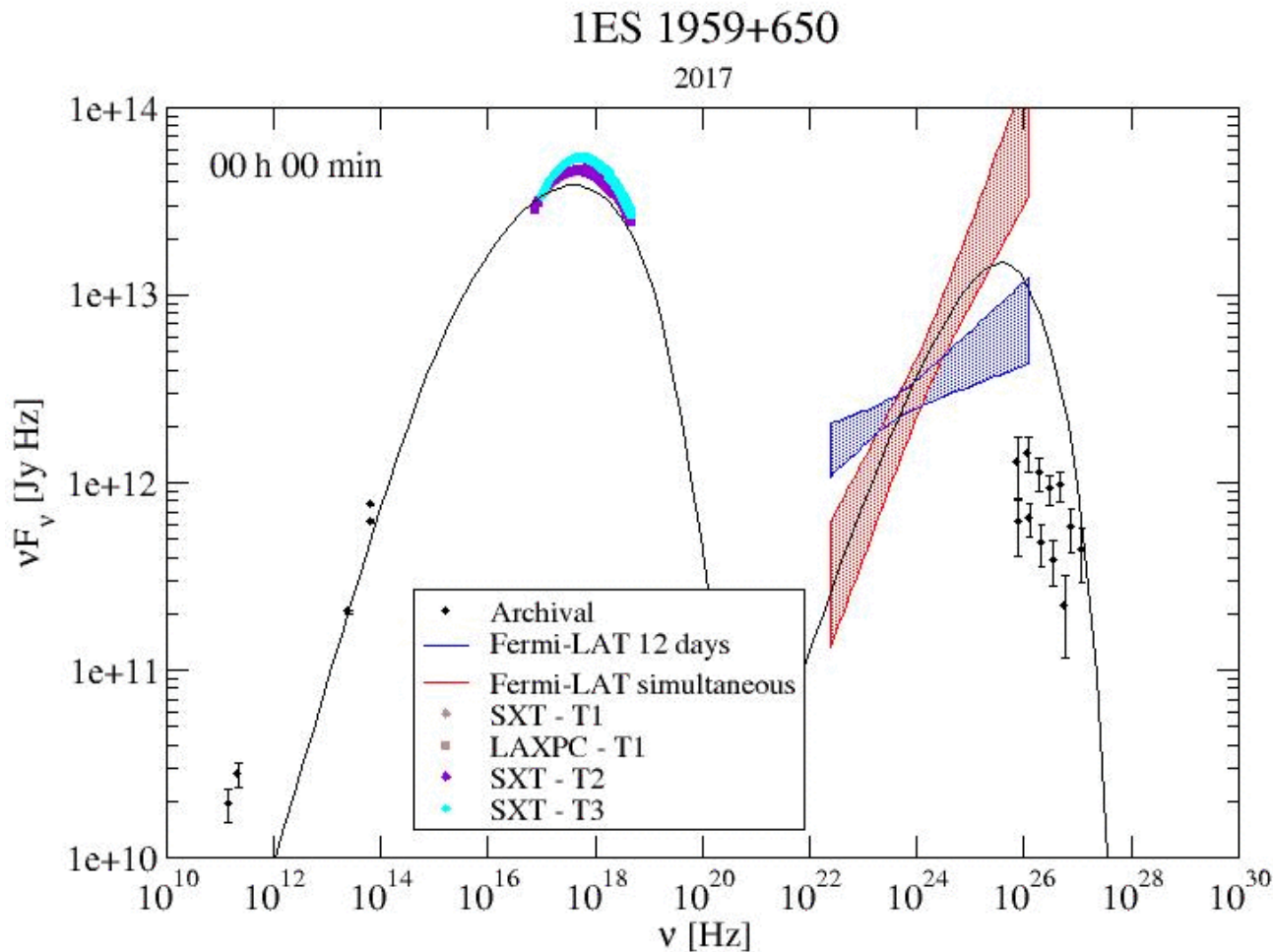
Harder-when-brighter trend without significant spectral hysteresis is well reproduced.

(Chandra et al. 2021)

1ES 1959+650 in 2017

Higher flux state well reproduced by changing Doppler factor
(smaller viewing angle θ_{obs} : $2.87^\circ \rightarrow 2.34^\circ$)

$$\lambda_{\text{pas}} = 40 r_g \gamma^{0.8}$$



(Chandra et al. 2021)

$$\eta_1 = 40$$

$$\alpha = 1.8$$

$$B = 0.08 \text{ G}$$

$$\delta = 24$$

$$R = 10^{16} \text{ cm}$$

$$\rightarrow \Delta t' \sim 3 \cdot 10^5 \text{ s}$$

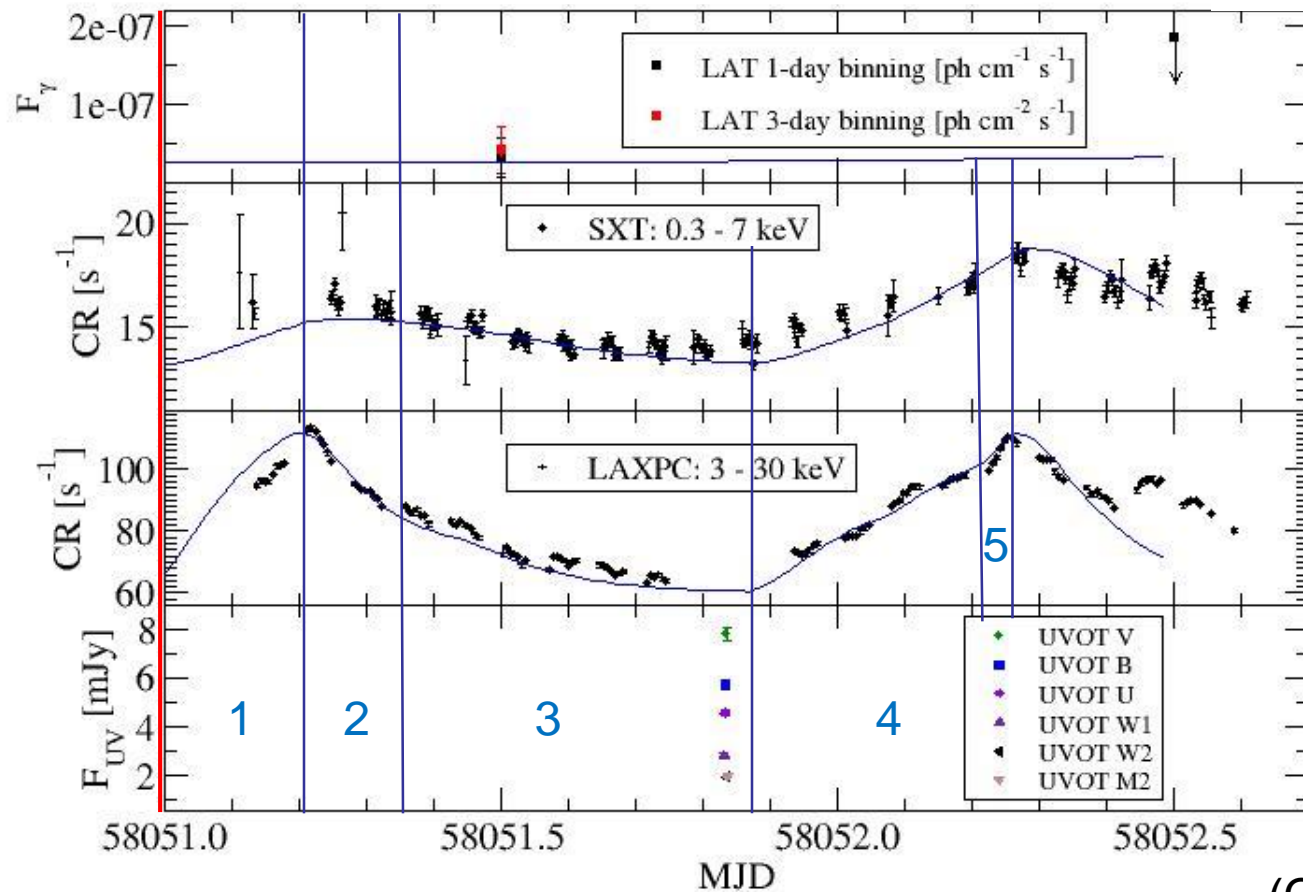
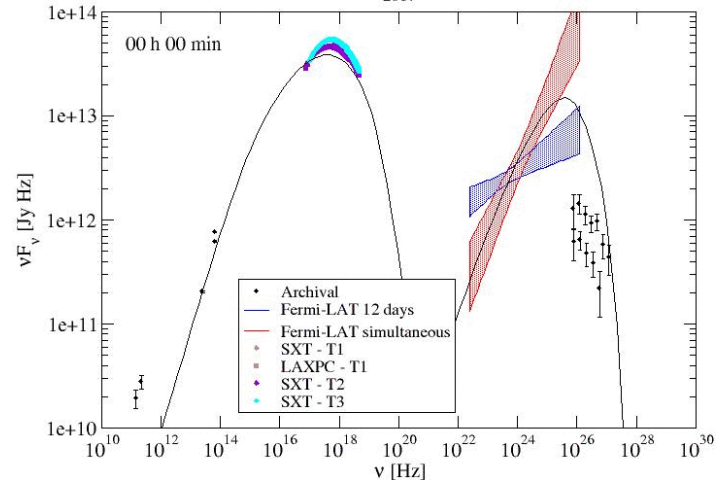
$$\rightarrow \Delta t_{\text{obs}} \sim 3.9 \text{ h}$$

Flaring caused by

- increasing L_{inj}
- decreasing η_0
- decreasing α

2017: MWL Light Curves

Parameter [units]	L_{inj} [erg/s]	η_0	α
Quiescence	2.8×10^{40}	40	1.8
Shock 1	3.5×10^{40}	30	1.7
Shock 2	3.0×10^{40}	30	1.8
Shock 3	3.6×10^{40}	25	1.8
Shock 4	4.3×10^{40}	25	1.8
Shock 5	5.1×10^{40}	15	1.8



(Chandra et al. 2021)

Summary

1. Coupled MC Simulations of Diffusive Shock Acceleration and radiation transport reveal strongly energy-dependent mean-free-path to pitch-angle scattering.
2. Time-dependent simulations of shock-in-jet model with realistic particle injection from diffusive shock acceleration, applied to long AstroSAT + MWL observations of 1ES 1959+650 in 2016 and 2017:
3. Flares with harder-when-brighter trend (no significant spectral hysteresis) well reproduced by decreasing pitch-angle-scattering mean-free path → increased turbulence levels induced by shock passage.



Thank you!



Based on Böttcher & Baring (2019): ApJ, 887, 133 (arXiv:1911.02834)
+ Chandra et al. (2021): ApJ, submitted

Any opinion, finding and conclusion or recommendation expressed in this material is that of the authors and the NRF does not accept any liability in this regard.